A New Parameterization for Entrainment in Overflows

CLAUDIA CENEDESE

Department of Physical Oceanography, Woods Hole Oceanographic Institution, Woods Hole, Massachusetts

CLAUDIA ADDUCE

Dipartimento di Scienze dell'Ingegneria Civile, Universita' RomaTre, Rome, Italy

(Manuscript received 30 September 2009, in final form 2 April 2010)

ABSTRACT

Dense overflows entrain surrounding waters at specific locations, for example, sills and constrictions, but also along the descent over the continental slope. The amount of entrainment dictates the final properties of these overflows, and thus is of fundamental importance to the understanding of the formation of deep water masses. Even when resolving the overflows, coarse resolution global circulation and climate models cannot resolve the entrainment processes that are often parameterized. A new empirical parameterization is suggested, obtained using an oceanic and laboratory dataset, which includes two novel aspects. First, the parameterization depends on both the Froude number (Fr) and Reynolds number of the flow. Second, it takes into account subcritical (Fr < 1) entrainment. A weak, but nonzero, entrainment can change the final density and, consequently, the depth and location of important water masses in the open ocean. This is especially true when the dense current follows a long path over the slope in a subcritical regime, as observed in the southern Greenland Deep Western Boundary Current. A streamtube model employing this new parameterization gives results that are more consistent with previous laboratory and oceanographic observations than when a classical parameterization is used. Finally, the new parameterization predictions compare favorably to recent oceanographic measurements of entrainment and turbulent diapycnal mixing rates, using scaling arguments to relate the entrainment ratio to diapycnal diffusivities.

1. Introduction

Dense waters are generated in several regions usually located at high latitude, where either strong atmospheric cooling and/or ice formation with consequent brine rejection, contribute to increasing the water density. These waters may flow over a sill or through a constriction to form dense currents descending the continental slope, hence the name overflows. Examples of locations of such overflows are the Denmark Strait (Dickson and Brown 1994; Girton and Sanford 2003; Käse et al. 2003), the Faroe Bank Channel (Saunders 1990; Mauritzen et al. 2005), the Baltic Sea (Arneborg et al. 2007), and various locations along the Arctic (Aagaard et al. 1981) and Antarctic (Muench et al. 2009; Padman et al. 2009; Foster and Carmack 1976) continental shelves. Marginal seas, where evaporation induces an increase in density, are other regions of dense water formation; for example, the Mediterranean (Baringer and Price 1997; Price et al. 1993), the Red Sea (Peters and Johns 2005; Peters et al. 2005), and the Persian Sea. Dense currents descend the continental slope for long distances before encountering the ocean bottom or interleaving at their level of neutral buoyancy. At the sill/constriction and during the descent, dense currents have been observed to entrain the surrounding ambient fluid. The final properties of their water masses are dictated by the amount and properties of the entrained fluid. Vertical profiles through the dense current have shown that the top of the current is a region with usually large velocity shear and low Richardson number, which presents large turbulent displacements indicative of entrainment due to shear-driven mixing (Figs. 2d,f of Peters and Johns 2005). The bottom of the dense current is also a region with a low Richardson number due to the large shear caused by frictional drag. Mixing occurring in this bottom region contributes to the dilution of the densest water mass, even if most of

Corresponding author address: Claudia Cenedese, Woods Hole Oceanographic Institution, 360 Woods Hole Rd., Woods Hole, MA 02536.
E-mail: ccenedese@whoi.edu

DOI: 10.1175/2010JPO4374.1

the entrainment is confined to the top of the current. Furthermore, Özgökmen and Fischer (2008) recently found that form drag resulting from separation around rough bottom topography can be as important as the bottom shear drag for the dynamics of the overflow. In the present study, we focus solely on the shear region at the top of the dense current, which we believe is driving the entrainment in most of the overflows examined. However, very shallow overflows whose height is comparable to the bottom boundary layer depth will be influenced by bottom friction, and the entrainment will be due to a combination of shear-mixing at the top and friction at the bottom of the current (Umlauf and Arneborg 2009a,b). Some overflows, like the one generated in the Ross Sea contributing to the formation of dense Antarctic Bottom Water (AABW), can be impacted by tidal currents that may affect the outflow volume transport and hydrographic properties. In the Ross Sea, tidal currents exceeding 1 m s^{-1} at spring tide advect water parcels 20 km across the continental slope during a half tidal cycle and have been observed to increase the benthic layer thickness (Padman et al. 2009). Dense currents are an integral part of the thermohaline circulation and their water properties are of global importance. For example, one of the most important sources of deep water in the oceans is the North Atlantic Deep Water (NADW), which is formed in the Nordic seas, and its water properties are modified by entrainment occurring at the Denmark Strait, Faroe Bank Channel, and along the descent over the continental slope.

The dynamics of dense currents have been thoroughly investigated in the past starting with Ellison and Turner (1959). Price and Baringer (1994) used an entrainment parameterization based on the results of Ellison and Turner (1959) in a streamtube model where the dense current flowed downslope balancing buoyancy, Coriolis, and friction forces. This model considered a motionless overlying ambient ocean and ignored any three-dimensional effects by laterally integrating over the streamtube. Jungclaus and Backhaus (1994) resolved the plume horizontally using a hydrostatic, reduced gravity, two-dimensional primitive equation numerical model. This latter study investigated the transient character of dense currents flowing down a slope and the effects of topographic disturbances. Recently, the importance of representing overflow dynamics in global circulation and climate models became apparent and led to a significant collaborative effort and formation of the so-called climate process team on gravity current entrainment (Legg et al. 2009). Coarse resolution does not allow these models to resolve the overflow regions; hence, the overflow dynamics are either oversimplified or ignored. An effort has been made to represent small passages with widths of order of 10 km, which connect source regions of dense water to the continental slope and the open ocean. Using the so-called ''partially open cell-faces'' (A. Adcroft and R. W. Hallberg 2004, personal communication), coarse resolution models can now resolve the overflows. However, these models still cannot resolve the entrainment processes that are consequently often parameterized. A widely used parameterization, based on the results of Ellison and Turner (1959), uses a supercritcal Froude number ($\mathrm{Fr} \geq 1$) criterion that assigns zero entrainment to subcritical flows. The entrainment velocity, $We = EU$, is considered to be a function of the local mean velocity of the flow U, and the entrainment parameter E is represented, based on the experiments of Ellison and Turner (1959) and subsequent analysis (Turner 1986), by

$$E = \begin{cases} \dfrac{0.08\mathrm{Fr}^2 - 0.1}{\mathrm{Fr}^2 + 5}, & \text{for} \quad \mathrm{Fr}^2 \geq 1.25 \\ 0, & \text{for} \quad \mathrm{Fr}^2 < 1.25 \end{cases}. \qquad (1)$$

The above expression was obtained assuming that the entire dense current is a single layer in which the properties are averaged within the layer depth and over the current cross section. Hence, the Froude number in Eq. (1) is a bulk property of the flow defined as $\mathrm{Fr} = \Delta U/\sqrt{Hg\Delta\rho/\rho_0}$, where g is the gravitational acceleration, H is the dense layer depth, ΔU and $\Delta\rho$ are the velocity and density difference between the dense current and the ambient fluid of density ρ_0. The entrainment is assumed to modify the water properties throughout the layer depth in the dense current.

In past years, active research has been focusing on the dynamics of overflows (Ezer 2005, 2006; Legg et al. 2006; Riemenschneider and Legg 2007; Özgökmen et al. 2006, 2009; Chang et al. 2008) and on finding new ways to better parameterize entrainment in dense overflows. Hallberg (2000) and Xu et al. (2006) parameterized entrainment into a dense current using expressions that included a function of Fr similar to Eq. (1). However, in isopycnic coordinate models, the dense current is represented by multiple layers, and the entrainment formulation is for a change in layer thickness because of a gradient Richardson number Ri, rather than a bulk Richardson number $\mathrm{Ri}_b = 1/\mathrm{Fr}^2$, which required the use of Ri instead of Ri_b in the expressions similar to Eq. (1). Their expressions present a critical gradient Richardson number, above which entrainment is zero, equal to 0.8 (Hallberg 2000) and 0.25 (Xu et al. 2006). Jackson et al. (2008) proposed a new parameterization for shear-driven mixing with particular focus on overflows. Their expression included a decay length scale to allow for turbulent eddies, generated in the low Ri layer, to be self-advected and mix in adjacent regions. Their expression maintained an

entrainment function $F(\mathrm{Ri})$ similar to Eq. (1) and suppressed entrainment above a critical Ri.

Rotating laboratory experiments carried out by Cenedese et al. (2004) and Cenedese and Adduce (2008), suggest that entrainment in dense currents can occur for subcritical Froude numbers, a fundamental difference from the Ellison and Turner (1959) parameterization, herein named the ET59 parameterization. Furthermore, a dependence of the entrainment on the Reynolds number was found by Cenedese and Adduce (2008). Wells and Wettlaufer (2005) reproduced the nonrotating results of Ellison and Turner (1959), and Wells (2007) found results similar to Ellison and Turner (1959) in rotating experiments. Nonrotating experiments investigating entrainment and detrainment in a dense current flowing downslope in a stratified fluid were conducted by Baines (2001, 2002, 2005, 2008) for different slope angles. The development of a dense current flowing down a slope in transition from a hydraulically controlled flow and the associate mixing and entrainment mechanisms have been investigated in the laboratory by Pawlak and Armi (2000).

2. A new parameterization

This study proposes a new parameterization for entrainment in dense currents flowing down a sloping bottom. The new parameterization takes into account the laboratory findings of Cenedese et al. (2004) and Cenedese and Adduce (2008). In particular, it assumes that the amount of entrainment in a dense current descending down a slope depends on both the Froude number Fr and Reynolds number Re of the flow and that entrainment occurs for subcritical Fr (<1). The subcritical entrainment observed in Cenedese et al. (2004) and Cenedese and Adduce (2008) has been suggested (Wåhlin and Cenedese 2006; Hughes and Griffiths 2006; Lauderdale et al. 2008) to be of fundamental importance for the water mass characteristics, such as density, of a dense current descending the continental slope. A weak, but nonzero, entrainment can change the final density and, consequently, the depth and location of important water masses in the open ocean. This is especially true when the dense current follows a long path over the slope in a subcritical regime. Lauderdale et al. (2008) found that moderate mixing rates in the southern Greenland Deep Western Boundary Current (DWBC) occurring over a distance of ~1000 km, between Denmark Strait and Cape Farewell, increase the volume transport of the dense current as much as the intense entrainment occurring near the sill in the Denmark Strait. Hence, the proposed new entrainment parameterization allows for subcritical Fr entrainment and takes into account the effects of both the Fr and Re on the entrainment dynamics. Consequently, the proposed parameterization differs substantially from the ET59 parameterization still widely used. The term ''entrainment'' is usually associated with the vigorous mixing due to Kelvin–Helmholtz instabilities in the shear layer of the dense current, which occurs typically near the sill, as the current descends a steep slope. In this study, as discussed in detail below, we use the term entrainment also to indicate the less energetic mixing occurring in the dense current as it descends the continental slope, with the possibility of including ''background'' mixing caused by, for example, internal waves breaking. The importance of subcritical Fr turbulent mixing in stably stratified flows has also been observed in data including meteorological observations, large eddy simulations, and direct numerical simulations. An improved second-order closure model accommodating arbitrary Richardson numbers has been proposed by Canuto et al. (2008).

The new parameterization has been obtained using a large dataset that includes oceanic and laboratory data. The oceanic data span five location sites: Mediterranean overflow (Baringer and Price 1997), Denmark Strait (Girton and Sanford 2003), Faroe Bank Channel (Mauritzen et al. 2005), Baltic Sea (Arneborg et al. 2007), and Lake Ogawara (Dallimore et al. 2001); while the laboratory data include both nonrotating (Ellison and Turner 1959; Alavian 1986) and rotating (Cenedese et al. 2004; Cenedese and Adduce 2008; Wells 2007) experiments on density driven currents descending a slope. For the majority of the data used, the values of the entrainment parameter, E, Fr, and Re are not ''local'' and ''instantaneous'' measurements, but instead are based on ''integral'' measurements. For example, the value of E is usually found by a mass balance between two consecutive sections across the dense current, similarly the values of Fr and Re are cross-sectional averages and/or averaged in time. Hence, the proposed parameterization should be used exclusively to predict an average value of E given the average values of Fr and Re across a section in the dense current. This parameterization is not meant to resolve, for example, the vertical changes in entrainment velocity due to vertical changes of the gradient Richardson number.

The mathematical structure of the suggested parameterization is similar to that proposed by Ellison and Turner (1959) and likewise is empirical,

$$E_{\mathrm{new}} = \frac{\mathrm{Min} + A\mathrm{Fr}^{\alpha}}{1 + AC_{\mathrm{inf}}(\mathrm{Fr} + \mathrm{Fr}_0)^{\alpha}}, \tag{2}$$

where Min, A, F_0, and α are constants and C_{inf} is given by

$$C_{\mathrm{inf}} = \frac{1}{\mathrm{Max}} + \left(\frac{B}{\mathrm{Re}^{\beta}}\right), \tag{3}$$

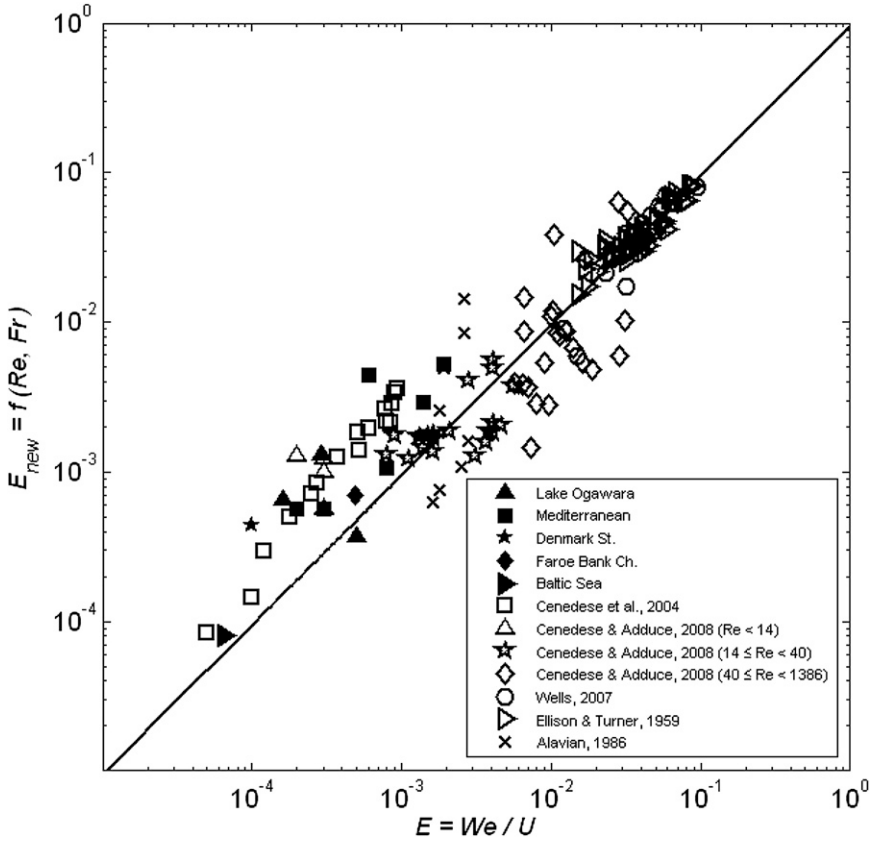

FIG. 1. Measured entrainment parameter E vs the entrainment parameter E_{new} given by Eq. (2). The solid line is the linear fit of the data given by the expression $E_{\text{new}} = 0.95E$ with an $R^2 = 0.91$. Solid (open) symbols indicate oceanic (laboratory) data.

where Max, B, and β are constants. For small Fr (i.e., $\text{Fr} \to 0$), Eq. (2) becomes $E_{\text{new}} = \text{Min}$,[1] while for $\text{Fr} \to \infty$, Eq. (2) becomes $E_{\text{new}} = 1/C_{\text{inf}}$ and for large Re (i.e., $\text{Re} \to \infty$) becomes $E_{\text{new}} = \text{Max}$. In the present study we choose the values of $\text{Min} = 4 \times 10^{-5}$ and $\text{Max} = 1$. The value $\text{Min} = 4 \times 10^{-5}$ is based on the limited oceanographic and laboratory data available for low Fr. The entrainment parameter obtained in the Baltic Sea (Arneborg et al. 2007) for $\text{Fr} = 0.55$ is close to the value observed in the laboratory by Cenedese et al. (2004) for a similar Fr. The availability of more oceanographic and laboratory data may modify the exact value of Min but, as discussed in detail in the next section, recent measurements of turbulent diapycnal mixing rates (Lauderdale et al. 2008) suggest that the value chosen for Min is representative of oceanic overflows with a low Fr. Unfortunately, oceanic data for large Fr are not available to the authors' knowledge. Hence, the value of Max is chosen more arbitrarily equal to 1, assuming that even for large Fr and Re, the entrainment parameter will reach an upper bound. The authors believe that, in the future, observational research should focus on collecting data at locations where large Fr are expected, to better define the upper bound of the entrainment parameter. A value of $E = 0.1$ was previously found for unstratified jets and plumes (ET59; Turner, 1986). For large Fr, the flow is driven by momentum rather than buoyancy forces, hence the upper bound $E = 0.1$, found for unstratified plumes, could also be employed. Given the lack of oceanic observations at large Fr and Re, which could help us choose between the two possible values of E for $\text{Fr} \to \infty$ and $\text{Re} \to \infty$, we choose arbitrarily $\text{Max} = 1$ with the understanding that new data and studies may lower this value down to $\text{Max} = 0.1$.

The other five constants in Eqs. (2) and (3) are determined by a nonlinear regression function, using least squares estimation, of the whole dataset to Eq. (2) giving $A = 3.4 \times 10^{-3}$, $F_0 = 0.51$, $\alpha = 7.18$, $B = 243.52$, and $\beta = 0.5$. Figure 1 shows the values of the entrainment parameter E_{new}, obtained using Eq. (2), versus the measured

[1] This is strictly true only if $AC_{\text{inf}}\text{Fr}_0^{\alpha} \ll 1$, which is the case for the constants' values found with the nonlinear regression function.

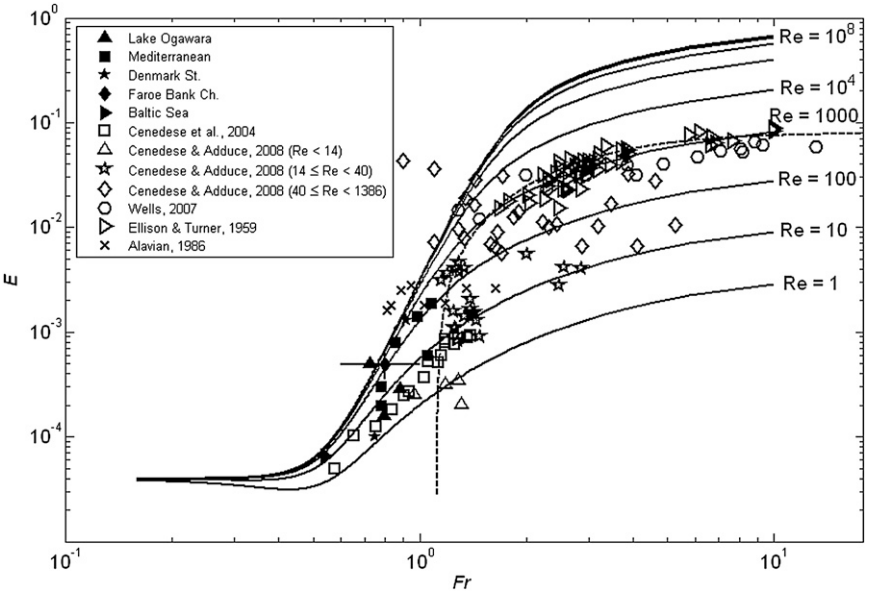

FIG. 2. Measured Fr vs E. The solid curves represent Eq. (2) for the different values of Re labeled on the rhs of the curves. The dashed line represents the ET59 parameterization given by Eq. (1). Solid (open) symbols indicate oceanic (laboratory) data.

entrainment E for the whole dataset. The values of Re used in (3) are $\mathrm{Re} = 10^7$ for the oceanic data (solid symbols), and for the laboratory experiments the Re quoted by the authors. The solid line represents the linear fit of the data, $E_{\mathrm{new}} = 0.95E$ with an $R^2 = 0.91$, and suggests that the new expression for the entrainment parameter is a very good representation of both the oceanic and laboratory data analyzed. Figure 2 shows the measured Fr and E for the dataset analyzed in the present study. The solid curves represent Eq. (2) for different values of Re. It is worth noting that the value of α is large, and the proposed parameterization has a strong dependence on the Fr around $\mathrm{Fr} = 1$. The ET59 parameterization (dashed line in Fig. 2) presents a subcritical Fr cutoff corresponding to a value of $\alpha \to \infty$ at $\mathrm{Fr}^2 = 1.25$. The new parameterization allows for subcritical Fr entrainment but maintains the strong dependence on Fr around $\mathrm{Fr} = 1$ observed both in the laboratory and oceanic dataset. The above results are only slightly modified when changing the values of Min and Max. For example, a value of $\mathrm{Max} = 0.5$ will produce a very similar fit between E and the predicted E_{new} as in Fig. 1, and the solid curves in Fig. 2 will be modified for $\mathrm{Fr} \to \infty$ and $\mathrm{Re} \to \infty$ to approach $E = 0.5$ instead of $E = 1$. A value of $\mathrm{Min} = 0$ will give the exact same fit between E and the predicted E_{new} as in Fig. 1, and the solid curves in Fig. 2 will be modified for $\mathrm{Fr} \lesssim 0.7$ and approach $E = 0$ instead of $E = 4 \times 10^{-5}$. The lack of data for both $\mathrm{Fr} \to \infty$ $\mathrm{Re} \to \infty$ and $\mathrm{Fr} \to 0$ explains why the proposed parameterization, derived by a nonlinear regression of the available oceanic and laboratory data, away from these limits is not strongly influenced by the choice of Min and Max.

The constants in Eq. (3) found by the nonlinear regression function suggest that Eq. (3) could be rewritten as

$$C_{\mathrm{inf}} = \frac{1}{\mathrm{Max}} + \left(\frac{\mathrm{Re}_{\mathrm{cr}}}{\mathrm{Re}}\right)^{1/2}, \tag{4}$$

where $\mathrm{Re}_{\mathrm{cr}} = 6 \times 10^4$ could represent the critical Re that must be exceeded to sustain three-dimensional inertially dominated turbulent fluctuations in a shear flow, which mark the so-called mixing transition (Dimotakis 2005). This transition is characterized by an increase in strain rates and area across which mixing occurs and, as a consequence, an increase in mixing activity occurs above $\mathrm{Re}_{\mathrm{cr}}$. The Re effects on the dynamics and mixing become substantially weaker with increasing Re, for $\mathrm{Re} > \mathrm{Re}_{\mathrm{cr}}$. Hence, we expect that the parameter E should increase and depend weakly on Re for $\mathrm{Re} > \mathrm{Re}_{\mathrm{cr}}$. Previous studies suggest values of $\mathrm{Re}_{\mathrm{cr}} = O(10^4)$ (Dimotakis 2005) and the value in Eq. (4) is within this range. Figure 2 supports the hypothesis that after approximately $\mathrm{Re}_{\mathrm{cr}} = 6 \times 10^4$ the value of the entrainment parameter is not strongly dependent on the Re, with the black curves being closer together. Although only speculation, it is interesting to note that the empirical fit of the oceanic and laboratory dataset may suggest the presence of a critical Re representing a mixing transition phenomena.

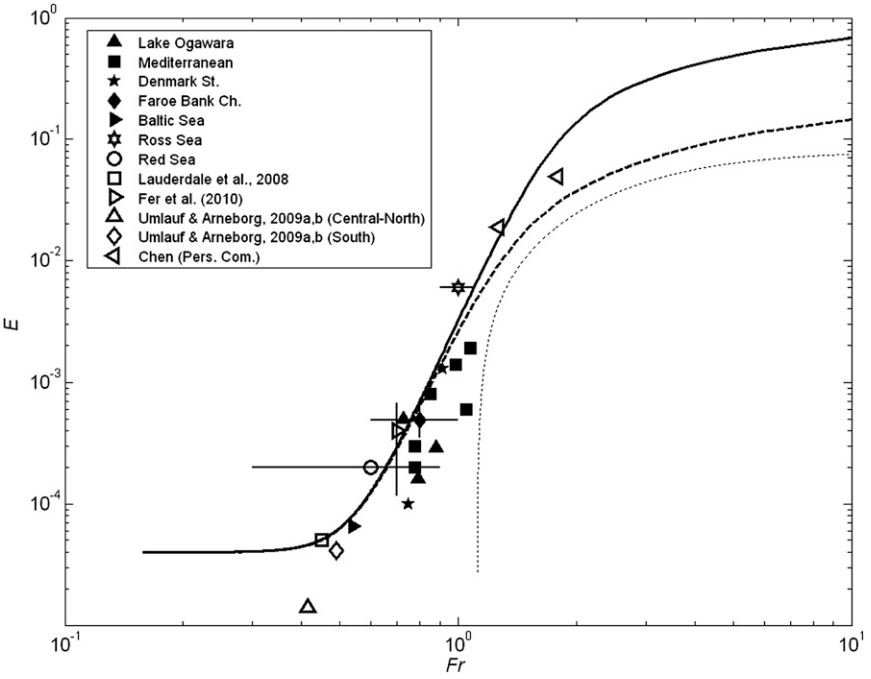

FIG. 3. Measured Fr vs E for the recent oceanic and laboratory measurements (open symbols) and the oceanic data shown in Fig. 2 (solid symbols). The solid (dashed) line represents the new parameterization, Eq. (2), obtained for Re = 10^8 (Re = 4000), while the dotted line represents the ET59 parameterization, Eq. (1). Error estimates are included when available.

The new entrainment parameterization does not directly include the effect of rotation. Cenedese and Adduce (2008) observed that rotational effects can cause the generation of cyclonic eddies above the dense current, as observed, for example, near the Denmark Strait overflow (Bruce 1995; Krauss 1996; Jungclaus et al. 2001). However, density measurements showed that eddies caused a very small amount of entrainment when compared to the entrainment in dense currents in the wave or turbulent regimes (Cenedese and Adduce 2008). Furthermore, rotational effects are expected to influence the trajectory of the dense current (i.e., the direction of the velocity vector), and the magnitude of the current velocity, ultimately influencing the values of Fr and Re. We believe that ''local'' mixing is not affected by rotation directly, but indirectly through the velocity magnitude and, consequently, the values of Fr and Re. This suggestion is supported by the rotating experiments of Wells (2007) that show values of the entrainment parameter basically indistinguishable from those obtained in the nonrotating experiments of Ellison and Turner (1959; Fig. 2). Hence, we do not include the effect of rotation directly in Eq. (2), with the understanding that rotation will influence the values of Fr and Re included in this expression.

Comparison with observations and laboratory data

To investigate how well the new parameterization predicts entrainment in overflows and dense currents, we now compare the values given by Eq. (2) with the direct estimates of entrainment for recent oceanographic measurements in overflows not included in the dataset used to derive Eq. (2). We use data obtained during the REDSOX field program in the Red Sea (Peters and Johns 2005; Peters et al. 2005), the Cross-Slope Exchanges at the Antarctic Slope Front (ANSLOPE) experiment in the Ross Sea (Muench et al. 2009), a dataset including hydrographic, current, and microstructure measurements from the western Baltic Sea (Umlauf and Arneborg 2009a,b), and a very recent dataset collected by Fer et al. (2010) in the Faroe Bank Channel. Furthermore, we also compare the new entrainment parameterization prediction with recent laboratory data obtained for large Re = 4000 by J. Chen (2009, personal communication). Figure 3 illustrates the value of E and Fr for these new datasets (open symbols), the oceanic observational data (solid symbols) shown in Fig. 2, the new parameterization, Eq. (2), obtained for Re = 10^8 (solid line) and Re = 4000 (dashed line), and the ET59 parameterization, Eq. (1) (dotted line). It should be noted that all

observed oceanic overflows present a subcritical Fr, for which the ET59 parameterization would predict zero entrainment. The new parameterization prediction of the entrainment parameter lies well within (Red Sea, Faroe Bank Channel) or very close to (Ross Sea) the error bars of the observational measurements.

The data from the western Baltic Sea (Umlauf and Arneborg 2009a,b) requires some caution since, as discussed in the introduction, dense currents having a small thickness compared to the bottom Ekman layer depth are strongly influenced by bottom friction. These recent cross-channel turbulence transects revealed a low mixing region (open triangle) on the central and northern slope, and a high mixing region (open diamond) on the southern slope, which could explain the large variability observed in the Arneborg et al. (2007) dataset obtained at a fixed location exactly between these two regions. However, the values of E obtained by Arneborg et al. (2007) (solid right triangle) are on average larger than those of Umlauf and Arneborg (2009a,b) reflecting a larger Fr, consistent with the prediction of the new parameterization. The high mixing rates on the southern slope (open diamond) observed by Umlauf and Arneborg (2009a,b) do not indicate local entrainment of ambient fluid, they indicate where ambient fluid entrained on the other side of the channel is finally mixed down within the dense current. The low mixing rates (open triangle), observed on the central and northern slope, indicate ambient fluid entrained in the interfacial boundary layer by the additional interfacial shear caused by the observed transverse circulation (Umlauf and Arneborg 2009a,b). The proposed parameterization is not meant to capture the effects of transverse circulation and friction in shallow overflows. It focuses solely on the shear region at the top of the dense current, which we believe is driving the entrainment into most of the overflows examined. Hence, it is not surprising that the new parameterization does not predict the entrainment rates measured in the western Baltic Sea, especially in the region affected by the transverse circulation (open triangle). Nevertheless, the comparison shown in Fig. 3, albeit done with only few observational data points, suggests that the new parameterization better represents entrainment in overflows when compared to previously used parameterizations that did not allow for subcritical mixing.

The laboratory data (open left triangles) obtained for large Re = 4000 by J. Chen (2009, personal communication) present slightly larger values of E than predicted by the new entrainment parameterization (dashed line). As in Cenedese and Adduce (2008), E is obtained using a mass balance between two cross sections of the dense current, but the values of Fr and Re were measured at the upstream cross section (source) and are not the average value between the two sections. Hence, Fr and Re represent "initial" values and not the values experienced by the dense current during the measured entrainment processes. This difference could partially explain the small discrepancy between the laboratory data (open left triangles) and the new parameterization prediction (dashed line), which, however, gives an improved prediction when compared to the ET59 parameterization (dotted line).

Unfortunately, oceanographic measurements of entrainment in overflows are not very common. To further test the new parameterization, we use some recent measurements of turbulent diapycnal mixing rates by Lauderdale et al. (2008). Diapycnal diffusivities K_ρ can be related to the vertical velocity using the steady-state advection–diffusion equation, where we assumed that the length scale of horizontal variations of the scalar T is much larger than that of vertical variation so that $\partial x, \partial y \ll \partial z$,

$$w\frac{\partial T}{\partial z} = K_\rho \frac{\partial^2 T}{\partial z^2}, \tag{5}$$

where w is the vertical velocity and T is a tracer, for example, temperature. By dimensional analysis, we obtain $w = K_\rho/L$, where L is a characteristic vertical length scale over which the tracer T presents gradients. Diapycnal diffusivities $K_\rho \sim 10^{-4}$ m^2 s^{-1} are common in the southern Greenland DWBC over the path between the Denmark Strait and Cape Farewell (~1000 km) and generate an increase in volume transport by entrainment similar to that occurring for the localized and more intense entrainment near the sill in the Denmark Strait, where $K_\rho \sim 10^{-3}$ m^2 s^{-1}. The large density gradients were observed (S. Bacon 2009, personal communication) to be confined within the dense current interface having a thickness of approximately 10 m, that is, L = 10 m, which yields a vertical velocity $w = 10^{-5}$ m s^{-1}. Hence, we find a value of the entrainment parameter $E = w/U = \frac{1}{2} \times 10^{-4}$, when using the measured dense current velocity $U = 0.2$ m s^{-1}. The value $\mathrm{Fr} = U/\sqrt{Hg\Delta\rho/\rho_0} = 0.45$ associated with the above entrainment parameter is obtained assuming a depth of the current $H = 200$ m and $\Delta\rho = 0.1$ kg m^{-3}. The open square in Fig. 3 represents the above estimates of E and Fr for the southern Greenland DWBC obtained using the turbulent diapycnal mixing rates recently observed by Lauderdale et al. (2008). The new parameterization does a very good job in representing the estimates of entrainment in a subcritical Fr overflow.

The value Min = 4×10^{-5}, which represents E_{new} for Fr $\rightarrow$ 0 in Eq. (2), is based on the limited available oceanic (Arneborg et al. 2007) and laboratory (Cenedese et al. 2004) data at low Fr. A finite value of E_{new} for Fr $\rightarrow$ 0 is preferred in order to include in this new parameterization

the entrainment and mixing due not only to shear instability occurring for moderate and high values of Fr, but also due to the so-called background mixing (Polzin et al. 1997) occurring at low values of Fr. By background mixing we refer to the mixing caused by, for example, internal waves breaking. Such mixing will undoubtedly contribute to small, but still finite, changes in the dense current properties. The background mixing has $K_\rho \sim 10^{-5} - 10^{-6}$ m^2 s^{-1} (Polzin et al. 1997), which with the above assumption $L = 10$ m and assuming also that $U = 0.1 - 0.01$ m s^{-1} for Fr $\rightarrow 0$ flows, gives an order of magnitude value for E between 10^{-4} and 10^{-6}. The average value $E \sim 10^{-5}$ is correctly represented by the new entrainment parameterization prediction for Fr $\rightarrow 0$, hence the proposed parameterization captures also the entrainment due to background mixing. On the contrary, one may choose to ignore the background mixing in this parameterization, and parameterize this mixing separately in general circulation and climate models. In this case, the value of Min = 0 and differences with the results discussed herein will arise only for Fr $\rightarrow 0$.

3. Streamtube model

A further test of the new parameterization given by Eq. (2) is performed using a streamtube model, similar to that of Price and Baringer (1994), to simulate the laboratory experiments of Cenedese and Adduce (2008), and the Mediterranean overflow data of Price and Baringer (1994). The momentum conservation equation for the dense overflow layer is

$$\frac{\partial \mathbf{U}}{\partial t} + \mathbf{U}\cdot\nabla\mathbf{U} + \mathbf{f}\times\mathbf{U} = \frac{g\Delta\rho\nabla D}{\rho_0} - \frac{\boldsymbol{\tau}_b}{\rho_0 H} - \frac{EU\mathbf{U}}{H}, \qquad (6)$$

where $\mathbf{U}$ is the dense layer velocity, $\mathbf{f}$ is the Coriolis parameter, D is the bottom depth, $\boldsymbol{\tau}_b = \rho_0 C_D U\mathbf{U}$ is the bottom stress, C_D is the drag coefficient, and E is the entrainment parameter. An important simplification is that the baroclinic pressure gradient arising from the alongstream variation of column height or density is assumed to be small in comparison with the buoyancy acceleration resulting from the density difference and bottom slope. We consider the linear steady-state solution of Eq. (6), hence ignoring the first two terms on the left-hand side. Finally, each numerical experiment is run twice, changing only the value of E that assumed the ET59 expression (1) in the first run, and the new proposed expression (2) in the second run.

a. Laboratory experiments

We choose two laboratory experiments with different Re from Cenedese and Adduce (2008) to investigate how the new parameterization predictions compare to those obtained using the ET59 parameterization. The streamtube model configuration is highly idealized to reproduce the geometry and initial conditions in the laboratory. The slope, $s = \nabla D$, is constant; the dense current is a single layer of density ρ; the ambient fluid is homogenous with a density ρ_0; the Coriolis parameter is constant (i.e., f plane); the initial flow rate of the dense current Q_0 is constant; and the initial width of the current is W_0, resulting in a initial velocity $U_0 = Q_0/H_0W_0$, where H_0 is the initial depth of the dense current. The values of the above parameters for the two laboratory experiments are shown in Table 1.

TABLE 1. Parameters used as initial conditions in the streamtube model. All values are in mks and temperature is in °C. Low (High) Re indicates the run shown in Fig. 5 (Fig. 6), and Med indicates the run shown in Fig. 8; S (S_0) and T (T_0) are the salinity and temperature of the dense (ambient) water and salinity is indicated only for the Med run. Here f_0 indicates the Coriolis parameter while $f = f_0 \cos\alpha$ (where α is the slope angle) is the vertical component of f_0 in the tilted coordinate frame used for the streamtube model. All other parameters are defined in the text.

Run	Low Re	High Re	Med
$\rho(S)$	1.0028×10^3	1.0022×10^3	(37.8)
$\rho_0(S_0)$	998.54	998.44	(35.7)
T	20	20	13.4
T_0	20	20	12
Q_0	2.5×10^{-6}	8.3×10^{-6}	1.5×10^6
f_0	1	1	8.4×10^{-5}
H_0	0.002	0.004	100
W_0	0.067	0.067	15×10^3
s	0.7	4.14	$12\ (4) \times 10^{-3}$
C_D	0.19	0.48	0.003

The width of the dense current, as it descends the slope, is imposed to be equal to that observed in the laboratory experiments. Price and Baringer (1994) suggested a parameterization for the broadening of the current which depends on the Ekman number. However, this parameterization was recently found (J. F. Price 2008, personal communication) inadequate to represent the broadening of several overflows, such as the Faroe Bank Channel overflow. The dynamics regulating the broadening of a dense current descending a slope are still unknown and a theory predicting either the width of the current as it descends the slope, or how the width depends on the external parameters, is still missing. Hence, we prefer to impose the evolution of the width of the current to be the same as observed in the laboratory. The height of the current, as it descends the slope, is computed taking into account the amount of entrained fluid. Finally, the value of the drag coefficient C_D is determined assuming that in the experiments of Cenedese and Adduce (2008) the angle θ between the flow trajectory and the alongslope

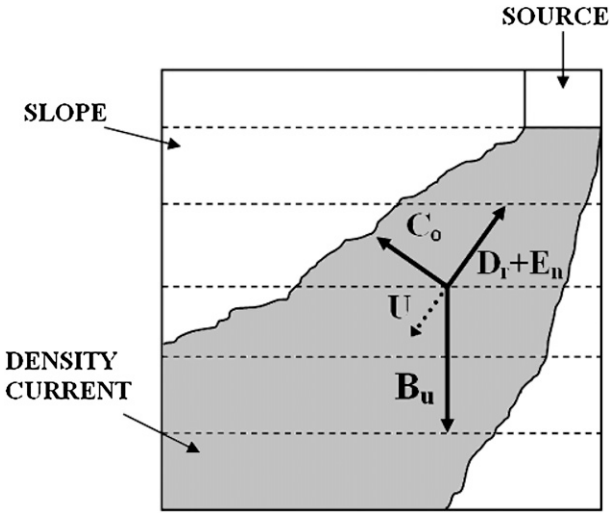

FIG. 4. Sketch of the forces acting on a dense current descending a sloping bottom in the presence of background rotation: Coriolis C_o, buoyancy B_u, drag D_r, and entrainment E_n. The resulting velocity is indicated by the dotted arrow. Dashed lines indicate isobaths.

direction ($S_t = \tan\theta$), is given by the ratio of the drag and Coriolis forces, as shown schematically in Fig. 4;

$$S_t = \frac{\text{Drag}}{\text{Coriolis}} = \frac{C_D U^2}{H}\frac{1}{fU}. \tag{7}$$

Hence, an expression for C_D in the laboratory can be obtained

$$C_D = \frac{S_t f H}{U}, \tag{8}$$

which, for the experiments of Cenedese and Adduce (2008), spans values between 0.1 and 0.7. Similar values of C_D were also found in the laboratory experiments of Ross et al. (2002). The model results' sensitivity to the choice of the drag coefficient has been examined and is discussed later in the text. Equation (7) assumes that $E \ll C_D$, which is the case for these experiments where $E = O(10^{-2} - 10^{-3})$.

Figures 5 and 6 show the results of the streamtube model calculation when using the new entrainment parameterization (solid curves) and the ET59 parameterization (dashed curves) and compare those to the laboratory measurements (triangles) of a low Re experiment (Re = 14.6; Fig. 5) and a high Re experiment (Re = 331.5; Fig. 6). As expected, the low Re and Fr experiments are better modeled when using the new entrainment parameterization E_{new} that takes into account a Re dependence of the entrainment and a subcritical Fr entrainment. In particular, the low Re experiment in Fig. 5 has a Fr = 1.5 for which the ET59 parameterization predicts a larger entrainment than observed in the laboratory. The ET59 parameterization was obtained by empirically fitting laboratory experiments having Re = $O(10^3)$ and does not take into account the Re dependence of the entrainment parameter observed by Cenedese and Adduce (2008). Hence, it is not surprising that it cannot correctly predict the entrainment for experiments with a Re very different from that of the ET59 experiments. The new parameterization predicts fairly well the decrease in density of the dense current as it descends the slope (Fig. 5a). The average current height measured in the experiment is well represented in the model when using the new parameterization (Fig. 5b), and on the opposite, the ET59 parameterization produces a height that is larger than observed because of the larger entrainment. Finally, when using E_{new}, the trajectory of the dense current as it descends the slope is closer to the observed trajectory than when using the ET59 parameterization (Fig. 5c). However, the velocity of the dense current is very similar when using the two different entrainment parameterizations, suggesting that the changes in density are balanced by the change in height of the current and not by a change in the velocity of the dense fluid. The dense current modeled velocities agree with those measured in the laboratory as shown in Fig. 5d.

As the Re of the experiment increases and reaches the same order as that in ET59 laboratory experiments, we expect the new parameterization to give similar results as the ET59 parameterization. Figure 6a shows how the density of the current descending the slope is predicted slightly better when using the new parameterization than the ET59, but the difference between the two predictions is small when compared to that observed for the low Re experiment (Fig. 5a). The current height measured in the laboratory lies in between the average height predicted by the two parameterizations (Fig. 6b), while the prediction of the velocity is very similar regardless of the parameterization used (Fig. 6d). Finally, for both parameterizations, the modeled trajectory is more downslope than the observed trajectory in the upper part of the slope (Fig. 6c). As the current descends, the ET59 parameterization predicts a trajectory with a larger alongslope component that better represents the final position of the dense current on the slope.

The sensitivity of the model results to the choice of the drag coefficient has been examined. The streamtube calculations of the low Re experiment illustrated in Fig. 5 have a value of $C_D = 0.19$ obtained using Eq. (8). The model is run with the same initial conditions, using the new entrainment parameterization, but with two other different values of the drag coefficient spanning two

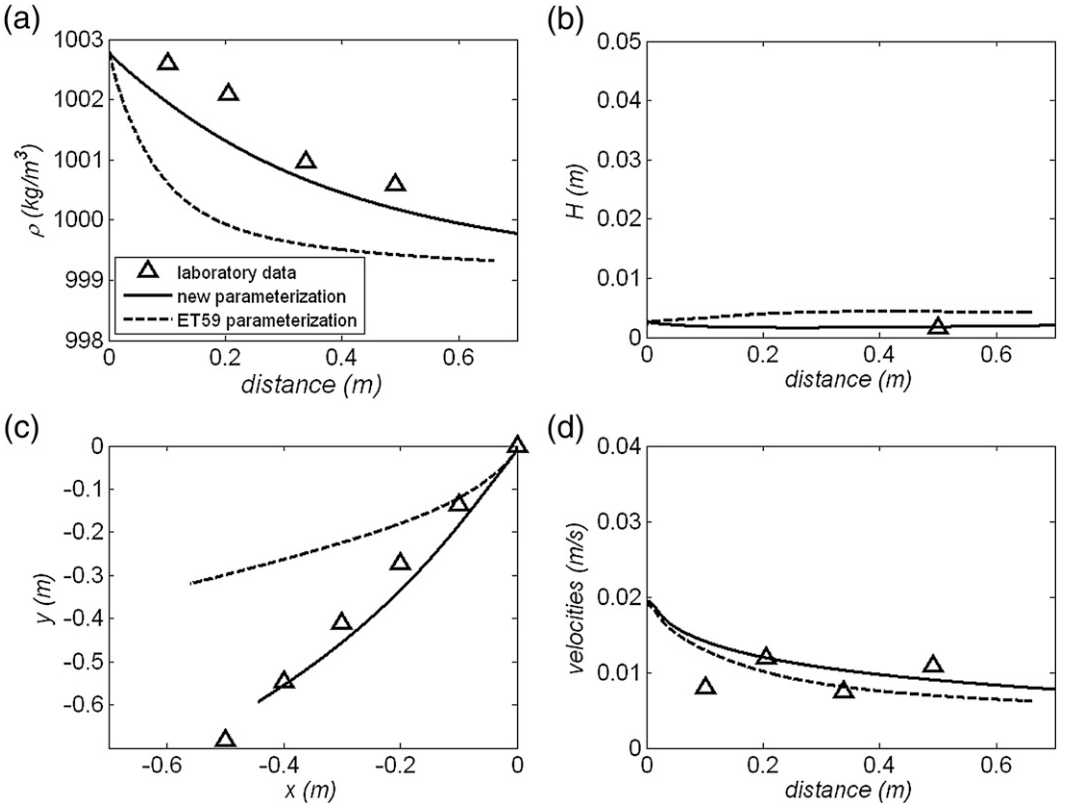

FIG. 5. Streamtube model calculations using the new entrainment parameterization (solid curves) and the ET59 parameterization (dashed curves) compared to the laboratory measurements (triangles) of a low Reynolds number experiment (Re = 14.6). (a) Density, (b) height, (c) trajectory, and (d) velocity of the dense current. The experimental value of the height is an average value over the whole current positioned arbitrarily at a distance from the source equal to 0.5 m.

orders of magnitude; that is, $C_D = 0.01$ and $C_D = 1$. As expected, a lower value of the drag coefficient causes a larger velocity of the dense current descending the slope and, consequently, a larger Fr and entrainment with a lower final density of the current. The current does not descend the slope as much as when employing larger values of C_D (Fig. 7). On the other hand, a larger value of C_D allows the current to descend the slope with a larger downslope component, with a smaller velocity and amount of entrainment, and with a consequent larger density at the bottom of the slope. For the lower value of the drag coefficient a weak meander pattern appears near the source (Figs. 7b,d) because of the mismatch between the imposed initial conditions and the ''preferred'' balanced state illustrated in Fig. 4 (Smith 1975). These meanders are damped downstream by the viscous drag and do not appear when the drag coefficient is larger. The sensitivity analysis of the streamtube model calculations to the value of the drag coefficient reveals that this parameter is of fundamental importance when predicting the final location and density of a dense current descending a slope, as also previously noted by Smith (1975). The use of Eq. (8) to determine the drag coefficient for the model runs reproducing the laboratory experiment of Cenedese and Adduce (2008) guarantees the use of a value of C_D dynamically consistent. When Eq. (8) cannot be used, particular care must be taken in the choice of C_D. One must be aware of the influence of the specific value used on the model results.

b. Mediterranean overflow

Streamtube model calculations are conducted to reproduce the Mediterranean overflow data of Price and Baringer (1994). The geometrical configuration of the model is kept the same as in the runs reproducing the laboratory experiments; that is, the bottom slope is constant, the ambient fluid has uniform density, and the dense current is homogenous. All the model parameters are chosen to be consistent with the data in Price and Baringer (1994) and are shown in Table 1. The slope is assumed to be gentler ($s = 4 \times 10^{-3}$) for the first 20 km, and after it assumes the value $s = 12 \times 10^{-3}$. The width

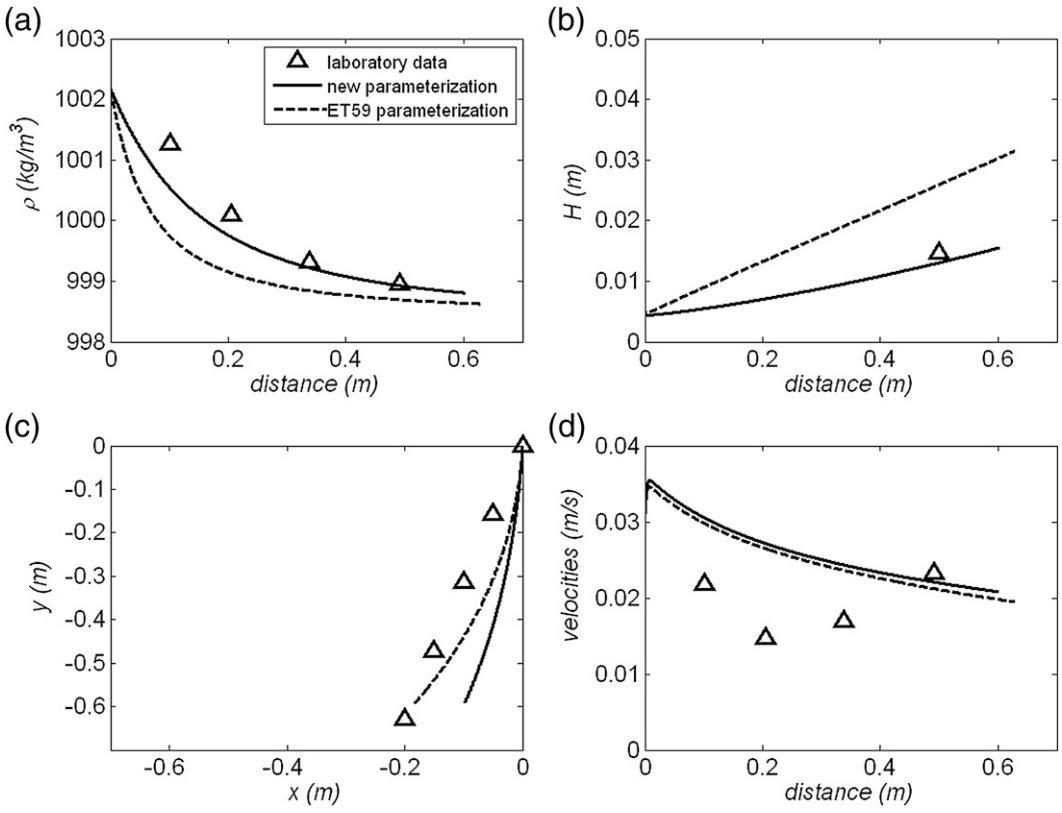

FIG. 6. Streamtube model calculations using the new entrainment parameterization (solid curves) and the ET59 parameterization (dashed curves) compared to the laboratory measurements (triangles) of a high Reynolds number experiment (Re = 331.5). (a) Density, (b) height, (c) trajectory, and (d) velocity of the dense current. The experimental value of the height is an average value over the whole current positioned arbitrarily at a distance from the source equal to 0.5 m.

of the dense current as it descends the slope is imposed to be consistent with the measurements in Fig. 7a of Price and Baringer (1994), and is parameterized as $W = W_0 + \gamma x$, where W_0 is the initial current width (Table 1), and $\gamma = 0.08$ for the first 20 km, and $\gamma = 0.3$ afterward (Fig. 8c).

The model results using the new parameterization (solid curves) and the ET59 parameterization (dashed curves) are shown in Fig. 8 where the triangles indicate the oceanographic measurements reported in Price and Baringer (1994). The streamtube model results obtained with the ET59 parameterization are very similar to those presented in Price and Baringer (1994). We do not expect an exact correspondence since the streamtube model of Price and Baringer (1994) included a detailed topography and a stratified ambient density profile. The similarity of the results indicates that the idealized model configuration used for the runs presented in Fig. 8 captures the main dynamics of the overflow, and the results are only slightly influenced by the details of the topography and the stratified ambient density profile.

The ET59 parameterization allows for entrainment only for supercritical Fr, that is, the values above the dotted line in Fig. 8b. Hence, the salinity of the dense current does not change until after ~30 km from the source. After this location, its value changes dramatically to reach $S = 36.5$ around 70 km, and remains almost unaltered for the rest of the descent over the slope since the Fr is subcritical until ~150 km and then it becomes barely critical. The new parameterization allows for subcritical Fr entrainment, and the dense current salinity is modified immediately after the source, with a smaller decrease in the first 30 km after the source, and a larger decrease between 30 and 70 km, as expected given the larger Fr (Fig. 8b). The results of the model using the two parameterizations are similar, both runs show a sudden decrease in salinity at the exit of the sill in the Strait of Gibraltar where the overflow is generated. However, with the new parameterization the entrainment begins at the source and the salinity at 70 km from the source is slightly lower than when using the ET59 parameterization. The most important difference

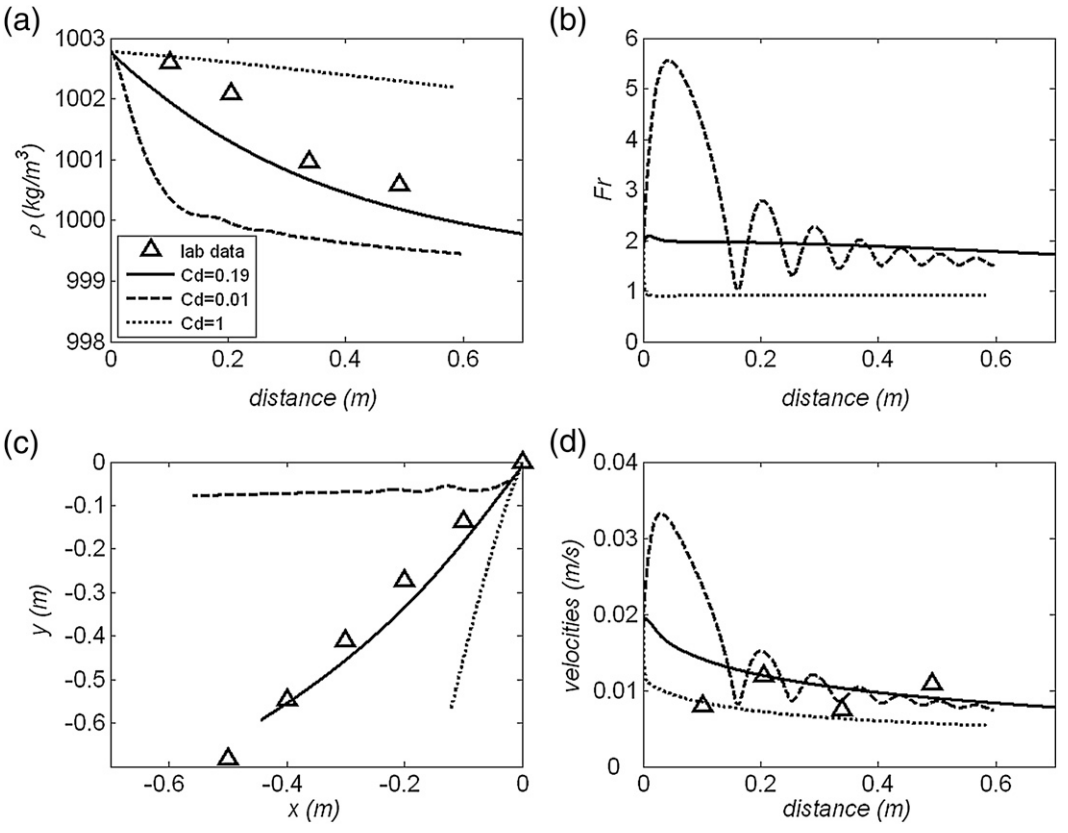

FIG. 7. Streamtube model calculations for the low Reynolds number experiment (Re = 14.6) shown in Fig. 5 using the new entrainment parameterization for three values of the drag coefficient: $C_D = 0.19$ (solid line), $C_D = 0.01$ (dashed line), and $C_D = 1$ (dotted line). The laboratory measurements are shown by the triangles. (a) Density, (b) Froude number, (c) trajectory, and (d) velocity of the dense current.

between the two parameterizations is apparent in the results after 70 km from the source. The ET59 parameterization does not allow for subcritical Fr entrainment, hence the final water properties of the dense current remain almost unchanged after 70 km from the source; that is, the density is almost constant during the descent over the continental slope. On the other hand, the new parameterization allows for subcritical Fr entrainment, and the salinity of the dense current continues to diminish along the descent, although at a rate much smaller than in the first 70 km. This weak entrainment influences the final salinity of the dense current, and explains the slight decrease in salinity observed in the data from 70 to 200 km (Fig. 8a). The dense current potential density measured after 250 km is 27.5 kg m^{-3} when using the new parameterization, and approximately 0.2 kg m^{-3} larger when using the ET59 parameterization. This difference in potential density corresponds approximately to a 250-m difference in the vertical location of these water masses when considering the ambient ocean potential density profile in Fig. 4b of Price and Baringer (1994). The difference in vertical location of the overflow water mass depends on the ambient stratification. Price and Baringer (1994) show that near the major overflows, the ambient stratification is quite weak at depth, the quoted Mediterranean overflow case presents one of the strongest ambient stratification. Hence, we expect that even a small difference in the final potential density of the overflow may cause a large difference in the vertical location of the overflow water mass. If one were to model a dense current descending the continental slope for a long distance in a subcritical Fr regime, the final properties and vertical location of the overflow water mass will differ dramatically depending on which parameterization is used.

The new parameterization gives a better prediction of the height of the dense current (Fig. 8d), while both parameterizations predict a realistic velocity within 50 km from the source and overestimate the current velocity after this location, with the new parameterization giving slightly lower values than the ET59 parameterization (Fig. 8f). The larger velocity and density obtained with the ET59 parameterization cause the dense current trajectory to have a larger downslope component than the

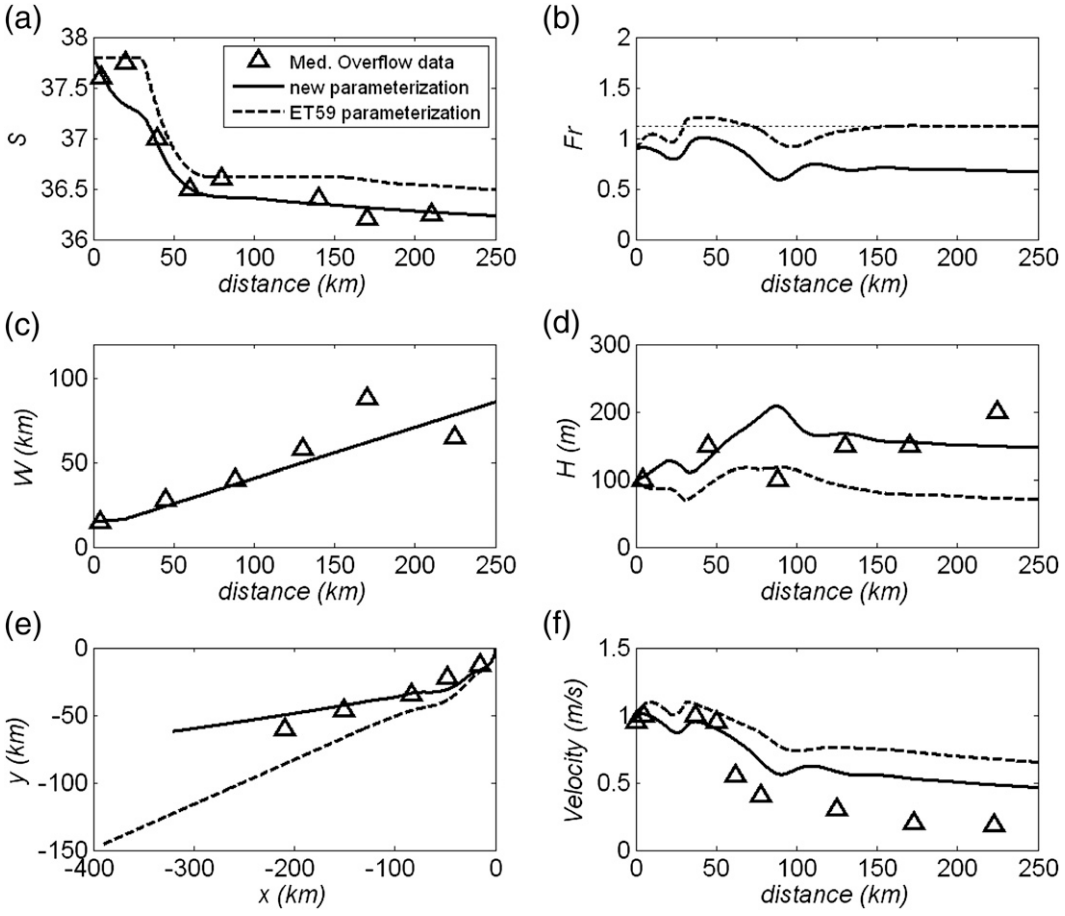

FIG. 8. Streamtube model calculations using the new entrainment parameterization (solid curves) and the ET59 parameterization (dashed curves) compared to the oceanic observations of the Mediterranean overflow (triangles) (Price and Baringer 1994). (a) Salinity, (b) Froude number, (c) width, (d) height, (e) trajectory, and (f) velocity of the dense current. The observed Mediterranean overflow trajectory is from Smith (1975).

trajectory predicted with the new parameterization, which compares very favorably with the observed trajectory of the Mediterranean overflow presented by Smith (1975). An exact correspondence between the predicted and observed path of the overflow is not expected due to the irregularities of the ocean bottom not represented in the model.

4. Conclusions

We propose a new parameterization for entrainment in overflows that takes into account the dependence of the entrainment on both the Fr and Re. The primary novelty of the proposed parameterization is that it allows for subcritical Fr entrainment. This is believed to be of major importance in the ocean since there are several locations where dense currents are observed to be subcritical but are still several hundreds of kilometers away from their neutrally buoyant level or the ocean bottom, suggesting that the final properties of these water masses are dictated by entrainment occurring at subcritical Fr. Furthermore, the proposed entrainment parameterization depends on the Re of the flow. This aspect is believed to be of importance not for the ocean itself, since the oceanic Re is very large and the Re dependence in Eq. (2) disappears for $\mathrm{Re} \to \infty$. However, when comparing laboratory data to oceanic observations, it is fundamentally important to understand, and take into account the entrainment dependence on the Re.

The new parameterization predictions compare favorably to recent oceanographic and laboratory measurements of entrainment. Streamtube model calculations show that the new parameterization, Eq. (2), leads to a significantly improved prediction of density, height, and trajectory of low Fr and Re laboratory experiments when compared to the predictions obtained using the ET59 parameterization. As expected, the two parameterizations give similar results for Re of the same order as those in the laboratory experiments of ET59.

The proposed parameterization has been obtained using a large dataset, which includes oceanic and laboratory data associated exclusively to dense currents and overflows. However, as discussed in Wells et al. (2010) the dependence of the entrainment parameter on the Froude number must be related to how efficiently stratified turbulence can convert the kinetic energy of the flow into irreversible mixing. Wells et al. (2010) propose an empirical relationship between the entrainment parameter E, the bulk Froude number Fr, and the flux coefficient Γ, hence suggesting the possibility that the proposed parameterization could be applicable not only to mixing in overflows, but also to other mixing mechanisms.

One aspect of the proposed parameterization is that the controlling nondimensional parameters Fr and Re are ''bulk'' properties of the dense flow. This choice was determined by the fact that, for the majority of the data used to obtain the new parameterization, the values of E, Fr, and Re are ''integral'' measurements. Hence, the proposed parameterization is able to predict an average value of E given the average diagnostic values of Fr and Re across a section in the dense current. However, most numerical models recently use entrainment parameterizations based on a local gradient Fr, or Ri (Hallberg 2000; Xu et al. 2006), which can be calculated pointwise. The entrainment in these models is sensitive to horizontal and vertical resolutions, indicating that the lack of resolution to capture criticality can be a possible concern when using a parameterization based on a local gradient Ri. Hence, the use of a local gradient Ri parameterization is not recommended for coarse-resolution global circulation and climate models (Xu et al. 2007). Recently, parameterizations for mixing in overflows based on second-order turbulent closure have been considered (Ilicak et al. 2008a,b, 2009). Provided fairly high-resolution regional models are used, most turbulence closure, in particular the so-called very large eddy simulation (VLES) technique, reproduce satisfactory ocean data from the Red Sea overflow (Ilicak et al. 2008a,b).

Finally, the present study focuses on the modification of the dense current properties by entrainment and illustrates the importance of a correct prediction of density to estimate the depth and location of important water masses in the open ocean. Another important quantity necessary to compute water mass production is the dense current transport and the modification it undergoes when entrainment occurs. Lauderdale et al. (2008) estimated an increase in volume transport by entrainment in the dense current over the path between the Denmark Strait and Cape Farewell similar to that occurring for the localized entrainment near the sill in the Denmark Strait. An estimate of the transport in a dense current can be obtained when one knows the entrainment rate between two consecutive sections across the dense current and the transport at the entering section. However, direct measurements of transport can be difficult and rare in the field. Often, the transport measurements along a dense current are not detailed enough to make a comparison with the estimate of increase in transport, especially on the open slope where the absence of topographic constrictions makes it particularly challenging to sample the entire fluid in a dense current. While this important aspect is clearly beyond the scope of this study, it certainly suggests that more field data are needed for dense overflows, not only near the sill or constriction where the overflows are generated, but also along the whole path such currents follow.

Acknowledgments. We wish to thank Mary-Louise Timmermans, Mathew Wells, Colm Caulfield, Lars Umlauf, and Jack Whitehead for invaluable discussions, Ilker Fer and Jun Chen for providing unpublished data, and Jason Hyatt for carefully reading drafts and substantially improving the clarity of the manuscript. Thanks are also given to R. Muench, S. Bacon, and one anonymous reviewer for their helpful comments on the manuscript. Support was given by the National Science Foundation Project OCE-0350891 and OCE-0726339.

REFERENCES

Aagaard, K., L. K. Coachman, and E. C. Carmack, 1981: On the halocline of the Arctic Ocean. *Deep-Sea Res.,* **28,** 529–545.

Alavian, V., 1986: Behavior of density currents on an incline. *J. Hydrol. Eng.,* **112,** 27–42.

Arneborg, L., V. Fiekas, L. Umlauf, and H. Burchard, 2007: Gravity current dynamics and entrainment—A process study based on observations in the Arkona Basin. *J. Phys. Oceanogr.,* **37,** 2094–2113.

Baines, P. G., 2001: Mixing in flows down gentle slopes into stratified environments. *J. Fluid Mech.,* **443,** 237–270.

——, 2002: Two-dimensional plumes in stratified environments. *J. Fluid Mech.,* **471,** 315–337.

——, 2005: Mixing regimes for the flow of dense fluid down slopes into stratified environments. *J. Fluid Mech.,* **538,** 245–267.

——, 2008: Mixing in downslope flows in the ocean–Plumes versus gravity currents. *Atmos.–Ocean,* **46,** 405–419.

Baringer, M. O., and J. F. Price, 1997: Mixing and spreading of the Mediterranean outflow. *J. Phys. Oceanogr.,* **27,** 1654–1677.

Bruce, J., 1995: Eddies southwest of the Denmark Strait. *Deep-Sea Res.,* **42,** 13–29.

Canuto, V. M., Y. Chen, A. M. Howardand, and I. N. Esau, 2008: Stably stratified flows: A model with no Ri(cr). *J. Atmos. Sci.,* **65,** 2437–2447.

Cenedese, C., and C. Adduce, 2008: Mixing in a density-driven current flowing down a slope in a rotating fluid. *J. Fluid Mech.,* **604,** 369–388.

——, J. A. Whitehead, T. A. Ascarelli, and M. Ohiwa, 2004: A dense current flowing down a sloping bottom in a rotating fluid. *J. Phys. Oceanogr.,* **34,** 188–203.

Chang, Y. S., T. M. Özgökmen, H. Peters, and X. Xu, 2008: Numerical simulation of the Red Sea outflow using HYCOM and comparison with REDSOX observations. *J. Phys. Oceanogr.,* **38,** 337–358.

Dallimore, C. J., J. Imberger, and T. Ishikawa, 2001: Entrainment and turbulence in saline underflow in Lake Ogawara. *J. Hydraul. Eng.,* **127,** 937–948.

Dickson, R. R., and J. Brown, 1994: The production of North Atlantic deep water: Sources, rates and pathways. *J. Geophys. Res.,* **99C,** 12 319–12 341.

Dimotakis, P. E., 2005: Turbulent mixing. *Annu. Rev. Fluid Mech.,* **37,** 329–356.

Ellison, T. H., and J. S. Turner, 1959: Turbulent entrainment in stratified flows. *J. Fluid Mech.,* **6,** 423–448.

Ezer, T., 2005: Entrainment, diapycnal mixing and transport in three-dimensional bottom gravity current simulations using the Mellor-Yamada turbulence scheme. *Ocean Modell.,* **9,** 151–168.

——, 2006: Topographic influence on overflow dynamics: Idealized numerical simulations and the Faroe Bank Channel overflow. *J. Geophys. Res.,* **111,** C02002, doi:10.1029/2005JC003195.

Fer, I., G. Voet, K. S. Seim, B. Rudels, and K. Latarius, 2010: Intense mixing of the Faroe Bank Channel overflow. *Geophys. Res. Lett.,* **37,** L026042, doi:10.1029/2009GL041924.

Foster, T. D., and E. C. Carmack, 1976: Frontal zone mixing and Antarctic Bottom Water formation in the southern Weddell Sea. *Deep-Sea Res.,* **23,** 301–317.

Girton, J. B., and T. B. Sanford, 2003: Descent and modification of the overflow plume in Denmark Strait. *J. Phys. Oceanogr.,* **33,** 1351–1364.

Hallberg, R. W., 2000: Time integration of diapycnal diffusion and Richardson number-dependent mixing in isopycnal coordinate ocean models. *Mon. Wea. Rev.,* **128,** 1402–1419.

Hughes, G. O., and R. W. Griffiths, 2006: A simple convective model of the global overturning circulation, including effects of entrainment into sinking regions. *Ocean Modell.,* **12,** 46–79.

Ilicak, M., T. M. Özgökmen, H. Peters, H. Z. Baumert, and M. Iskandarani, 2008a: Very large eddy simulation of the Red Sea overflow. *Ocean Modell.,* **20,** 183–206.

——, ——, ——, ——, and ——, 2008b: Performance of two-equation turbulence closures in three-dimensional simulations of the Red Sea overflow. *Ocean Modell.,* **24,** 122–139.

——, ——, E. Özsoy, and P. F. Fischer, 2009: Non-hydrostatic modeling of exchange flows across complex geometries. *Ocean Modell.,* **29,** 159–175.

Jackson, L., R. W. Hallberg, and S. Legg, 2008: A parameterization of shear-driven turbulence for ocean climate models. *J. Phys. Oceanogr.,* **38,** 1033–1053.

Jungclaus, J. H., and J. O. Backhaus, 1994: Application of a transient reduced gravity plume model to the Denmark Strait overflow. *J. Geophys. Res.,* **99C,** 12 375–12 396.

——, J. Hauser, and R. H. Käse, 2001: Cyclogenesis in the Denmark Strait overflow plume. *J. Phys. Oceanogr.,* **31,** 3214–3229.

Käse, R. H., J. B. Girton, and T. B. Sanford, 2003: Structure and variability of the Denmark Strait Overflow: Model and observations. *J. Geophys. Res.,* **108,** 3181, doi:10.1029/2002JC001548.

Krauss, W., 1996: A note on overflow eddies. *Deep-Sea Res.,* **43,** 1661–1667.

Lauderdale, J. M., S. Bacon, A. C. Naveira Garabato, and N. P. Holliday, 2008: Intensified turbulent mixing in the boundary current system of Southern Greenland. *Geophys. Res. Lett.,* **35,** L04611, doi:10.1029/2007GL032785.

Legg, S., R. W. Hallberg, and J. B. Girton, 2006: Comparison of entrainment in overflows simulated by z-coordinate, isopycnal and nonhydrostatic models. *Ocean Modell.,* **11,** 69–97.

——, and Coauthors, 2009: Improving oceanic overflow representation in climate models: The Gravity Current Entrainment Climate Process Team. *Bull. Amer. Meteor. Soc.,* **90,** 657–670.

Mauritzen, C., J. Price, T. Sanford, and D. Torres, 2005: Circulation and mixing in the Faroese Channels. *Deep-Sea Res. II,* **52,** 883–913.

Muench, R., L. Padman, A. Gordon, and A. Orsi, 2009: A dense water outflow from the Ross Sea, Antarctica: Mixing and the contribution of tides. *J. Mar. Syst.,* **77,** 369–387.

Özgökmen, T. M., and P. F. Fischer, 2008: On the role of bottom roughness in overflows. *Ocean Modell.,* **20,** 336–361.

——, ——, and W. E. Johns, 2006: Product water mass formation by turbulent density currents from a high-order nonhydrostatic spectral element model. *Ocean Modell.,* **12,** 237–267.

——, T. Iliescu, and P. F. Fischer, 2009: Reynolds number dependence of mixing in a lock-exchange system from direct numerical and large eddy simulations. *Ocean Modell.,* **30,** 190–206.

Padman, L., S. L. Howard, A. Orsi, and R. Muench, 2009: Tides of the northwestern Ross Sea and their impact on dense outflows of Antarctic Bottom Water. *Deep-Sea Res. II,* **56,** 818–834.

Pawlak, G., and L. Armi, 2000: Mixing and entrainment in developing stratified currents. *J. Fluid Mech.,* **424,** 45–73.

Peters, H., and W. E. Johns, 2005: Mixing and entrainment in the Red Sea outflow plume. Part II: Turbulence characteristics. *J. Phys. Oceanogr.,* **35,** 584–600.

——, ——, A. S. Bower, and D. M. Fratantoni, 2005: Mixing and entrainment in the Red Sea outflow plume. Part I: Plume structure. *J. Phys. Oceanogr.,* **35,** 569–583.

Polzin, K. L., J. M. Toole, J. R. Ledwell, and R. W. Schmitt, 1997: Spatial variability of turbulent mixing in the abyssal ocean. *Science,* **276,** 93–96.

Price, J. F., and M. O. Baringer, 1994: Outflows and deep water production by marginal seas. *Prog. Oceanogr.,* **33,** 161–200.

——, and Coauthors, 1993: Mediterranean outflow mixing and dynamics. *Science,* **259,** 1277–1282.

Riemenschneider, U., and S. Legg, 2007: Regional simulations of the Faroe Bank Channel overflow in a level model. *Ocean Modell.,* **17,** 93–122, doi:10.1016/j.ocemod.2007.01.003.

Ross, A. N., P. F. Linden, and S. B. Dalziel, 2002: A study of three-dimensional gravity currents on a uniform slope. *J. Fluid Mech.,* **453,** 239–261.

Saunders, P. M., 1990: Cold outflow from the Faroe Bank Channel. *J. Phys. Oceanogr.,* **20,** 29–43.

Smith, P. C., 1975: A streamtube model for bottom boundary currents in the ocean. *Deep-Sea Res.,* **22,** 853–873.

Turner, J. S., 1986: Turbulent entrainment: The development of the entrainment assumption and its application to geophysical flows. *J. Fluid Mech.,* **170,** 431–471.

Umlauf, L., and L. Arneborg, 2009a: Dynamics of rotating shallow gravity currents passing through a channel. Part I: Observation of transverse structure. *J. Phys. Oceanogr.,* **39,** 2385–2401.

——, and ——, 2009b: Dynamics of rotating shallow gravity currents passing through a channel. Part II: Analysis. *J. Phys. Oceanogr.,* **39,** 2402–2416.

Wåhlin, A. K., and C. Cenedese, 2006: How entraining density currents influence the ocean stratification. *Deep-Sea Res. II,* **53,** 172–193.

Wells, M. G., 2007: Influence of Coriolis forces on turbidity currents and sediment deposition. *Particle-Laden Flow: From Geophysical to Kolmogorov Scales,* B. J. Geurts, H. Clercx, and W. Uijttewaal, Eds., ERCOFTAC Series, 331–343.

——, and J. S. Wettlaufer, 2005: Two-dimensional density currents in a confined basin. *Geophys. Astrophys. Fluid Dyn.,* **99,** 199–218.

——, C. Cenedese, and C. P. Caulfield, 2010: The relationship between flux coefficient gamma and entrainment ratio *E* in density currents. *J. Phys. Oceanogr.,* in press.

Xu, X., Y. S. Chang, H. Peters, T. M. Özgökmen, and E. P. Chassignet, 2006: Parameterization of gravity current entrainment for ocean circulation models using a high-order 3D nonhydrostatic spectral element model. *Ocean Modell.,* **14,** 19–44.

——, E. P. Chassignet, J. F. Price, T. M. Özgökmen, and H. Peters, 2007: A regional modeling study of the entraining Mediterranean outflow. *J. Geophys. Res.,* **112,** C12005, doi:10.1029/2007JC004145.